Energy Fuels **2010,** *24,* 2667–2674 · DOI:10.1021/ef901427g
Published on Web 03/11/2010

energy&fuels
article

Measurement and Modeling of Biodiesel Cold-Flow Properties

João A. P. Coutinho,*,† M. Gonçalves,† M. J. Pratas, M. L. S. Batista,† V. F. S. Fernandes,† J. Pauly,‡ and J. L. Daridon‡

†*Departamento de Química, Centro de Investigação em Materiais Cerâmicos e Compósitos (CICECO), Universidade de Aveiro, 3810-193 Aveiro, Portugal, and* ‡*Laboratoire des Fluides Complexes, Centre Universitaire de Recherche Scientifique, Université de Pau, Avenue de l'Université, BP 1155, 64013 Pau, France*

Received November 23, 2009. Revised Manuscript Received February 15, 2010

Despite their interest for the understanding of the low-temperature behavior of biodiesel, data on the phase equilibria of biodiesels at temperatures below the cloud point are not available in the literature. To overcome this limitation, the liquid- and solid-phase compositions and fractions at temperatures below the cloud point were studied for three commercial diesels at temperatures ranging from 260 to 275 K. A thermodynamic framework able to describe these multiphase systems is presented. Two versions of the predictive UNIQUAC model along with an approach assuming complete immiscibility of the compounds in the solid phase are evaluated with success against the experimental phase equilibrium data measured in this work.

1. Introduction

Biodiesel production and consumption has been increasing steadily in the past few years thanks to the environmental benefits that result from its use. The cost of the raw materials and the competition with food for oils or soils are the main limitations to a more widespread use of biodiesel. The use of waste oil or cheap and non-edible oils and fats can help minimize this problem, but the formulation of a biodiesel must conform to a number of standards before approval for commercialization.

The main biodiesel properties are dependent upon the oils or fats used in its production. This biofuel is much less complex than conventional diesels. It consists of a liquid blend of non-toxic, biodegradable fatty acid esters, yellow colored and immiscible with water. Its cold-flow performance depends upon both the oil and the alcohol used in the transesterification. A biodiesel with a large concentration of saturated fatty acid esters, although less vulnerable to oxidation and displaying better combustion properties, has a worst performance at low temperatures because of its tendency to crystallize.[1] There are a number of specifications for the biodiesel performance at low temperatures. The most important are the cloud point (CP), the pour point (PP), the cold-filter plugging point (CFPP), and the low-temperature filterability test (LTFT).[2] Dunn and co-workers have produced a large body of work that provides a comprehensive picture of the influence of the saturated fatty esters and various alcohols on the low-temperature behavior of biodiesel.[1,3−8] What currently lacks is a good and reliable model that, from the knowledge of the biodiesel composition, could predict the low-temperature behavior of the fuel.[8] This model would be an essential tool for a quick evaluation of the biodiesel characteristics, design of a biodiesel to meet the requirements for low-temperature use, and design and operation of winterization processes for biodiesels.[9]

Our previous work has addressed the low-temperature behavior of conventional fuels. A thermodynamic model, predictive UNIQUAC,[10−15] was developed and extensively tested in diesels,[16−18] jet fuels and other refined products,[17,19−21] and unrefined oils[22−25] with success. Lately, we have been

*To whom correspondence should be addressed. E-mail: jcoutinho@ua.pt.

(1) Dunn, R. O.; Bagby, M. O. *J. Am. Oil Chem. Soc.* **1995**, *72*, 895–904.
(2) American Society for Testing and Materials (ASTM). *Annual Book of ASTM Standards*; ASTM: West Conshohocken, PA, 1999; Vol. 05.01.
(3) Dunn, R. O.; Shockley, M. W.; Bagby, M. O. *J. Am. Oil Chem. Soc.* **1996**, *73*, 1719–1728.
(4) Foglia, T. A.; Nelson, L. A.; Dunn, R. O. *J. Am. Oil Chem. Soc.* **1997**, *74*, 951–955.
(5) Dunn, R. O.; Bagby, M. O. *J. Am. Oil Chem. Soc.* **2000**, *77*, 1315–1323.
(6) Dunn, R. O. *J. Am. Oil Chem. Soc.* **2002**, *79*, 709–715.
(7) Dunn, R. O. *J. Am. Oil Chem. Soc.* **2008**, *85*, 961–972.
(8) Dunn, R. O. *Energy Fuels* **2009**, *23*, 4082–4091.
(9) Knothe, G. *Energy Fuels* **2008**, *22*, 1358–1364.
(10) Coutinho, J. A. P.; Knudsen, K.; Andersen, S. I.; Stenby, E. H. *Chem. Eng. Sci.* **1996**, *51*, 3273–3282.
(11) Coutinho, J. A. P.; Stenby, E. H. *Ind. Eng. Chem. Res.* **1996**, *35*, 918–925.
(12) Coutinho, J. A. P.; Ruffier-Meray, V. *Ind. Eng. Chem. Res.* **1997**, *36*, 4977–4983.
(13) Coutinho, J. A. P. *Ind. Eng. Chem. Res.* **1998**, *37*, 4870–4875.
(14) Coutinho, J. A. P. *Fluid Phase Equilib.* **1999**, *158−160*, 447–457.
(15) Coutinho, J. A. P.; Mirante, F.; Pauly, J. *Fluid Phase Equilib.* **2006**, *247*, 8–17.
(16) Coutinho, J. A. P.; Dauphin, C.; Daridon, J. L. *Fuel* **2000**, *79*, 607–616.
(17) Coutinho, J. A. P. *Energy Fuels* **2000**, *14*, 625–631.
(18) Pauly, J.; Daridon, J. L.; Sansot, J. M.; Coutinho, J. A. P. *Fuel* **2003**, *82*, 595–601.
(19) Mirante, F. I. C.; Coutinho, J. A. P. *Fluid Phase Equilib.* **2001**, *180*, 247–255.
(20) Coutinho, J. A. P.; Mirante, F.; Ribeiro, J. C.; Sansot, J. M.; Daridon, J. L. *Fuel* **2002**, *81*, 963–967.
(21) Queimada, A. J. N.; Dauphin, C.; Marrucho, I. M.; Coutinho, J. A. P. *Thermochim. Acta* **2001**, *372*, 93–101.
(22) Coutinho, J. A. P.; Daridon, J. L. *Energy Fuels* **2001**, *15*, 1454–1460.
(23) Daridon, J. L.; Pauly, J.; Coutinho, J. A. P.; Montel, F. *Energy Fuels* **2001**, *15*, 730–735.
(24) Sansot, J. M.; Pauly, J.; Daridon, J. L.; Coutinho, J. A. P. *AIChE J.* **2005**, *51*, 2089–2097.
(25) Coutinho, J. A. P.; Edmonds, B.; Morwood, T.; Szczepanski, B.; Zhang, X. *Energy Fuels* **2006**, *20*, 1081–1088.

addressing the application of this model to the description of the CPs of fatty acid mixtures[26] and fatty acid methyl[27] and ethyl ester[28] mixtures. The predictive UNIQUAC model was shown to be able to successfully describe the CP of the mixtures studied but presented limited advantages compared to a simpler model, where no solid solution formation was considered, as discussed in a previous work.[28]

The CP provides, however, limited information about the low-temperature behavior of a fuel. Both the CFPP and the LTFT are related to what happens below the CP, i.e., the composition of the material that precipitates and the amount of crystals formed. This last issue is particularly relevant because the gelling of the fluid and the plugging of filters is essentially dependent upon the amount of solids crystallizing at low temperatures. The adequate design and operation of winterization processes to produce biodiesel that can conform to low-temperature specifications also require the capability to predict the composition of the liquid phase after partial crystallization of a biodiesel and the prediction of its new low-temperature characteristics.[9,29−31] To learn more about the behavior of a biodiesel below its CP, an approach successfully used previously for the study of conventional diesels[16,18] and other complex synthetic mixtures[12,32−36] was applied here to biodiesels. It consists of separating by filtration the liquid and solid phases at various temperatures below the CP and studying their composition and relative amounts.

In this work, experimental data for the solid−liquid-phase equilibria of three commercial, non-additive biodiesels at temperatures ranging from 260 to 275 K are reported. A thermodynamic framework able to describe these multiphase systems is presented. Two versions of the predictive UNIQUAC model along with a model assuming complete immiscibility of the compounds on the solid phase are evaluated with success against the experimental data as shown below.

2. Experimental Section

The three commercial biodiesels studied here, BDA, BDB, and BDC, were obtained from Portuguese biodiesel-producing companies. They were collected at the end of the production line before additivation, and their composition was measured by gas chromatography on a Varian 3800CP chromatograph equipped with a split/splitless injector at 250 °C (split ratio of 1:20) and a flame ionization detector (FID) at 220 °C. A DB1-HT column (length, 15 m; internal diameter, 0.32 mm; and film thickness, 0.1 μm) coated with a film of dimethylpolysiloxane, with a temperature program of 5 °C/min from 80 to 200 °C, was used.

Table 1. Composition (wt %) and CPs of the Biodiesel Studied

	BDA	BDB	BDC
C16:0	16.18	5.59	11.04
C18:0	3.82	2.39	4.07
C18:1	28.80	55.20	22.92
C18:2	50.46	34.89	61.03
CP (K)	280	271	276

The carrier gas was helium, with a flow rate of 2 mL/min. The compositions of the fatty acid esters present in concentrations above 0.5 wt % are reported in Table 1. The total concentration of other esters was less than 2 wt %.

The low-temperature behavior of the biodiesels was studied using a methodology previously developed by us to measure solid−liquid-phase equilibria in hydrocarbon fluids[12,32] and widely used to study both synthetic mixtures[12,33−36] and diesels.[16,18] It consists of separating the liquid phase from the precipitate by filtration at a controlled temperature and analyzing the phases by gas chromatography. The phase separation is achieved using UniPrep syringeless filters from Whatman of 5 mL capacity with filters of 0.2 μm porosity. The biodiesel is distributed in 1 mL samples by the UniPrep that are introduced on a thermostatic bath, where the samples are equilibrated for 24 h before separation. When the separation is completed, the two phases recovered are analyzed using the gas chromatography analytical procedure described above. The liquid- and solid-phase composition and fractions are estimated by mass balances from the results of these analysis according to a procedure proposed previously[12,32] and detailed below. No multiple measurements were carried out for each point; therefore, a correct value of reproducibility of the experimental data cannot be assigned. On the basis of our previous experience[12,32−36] and on the results for the points that were duplicated, the estimated reproducibility is 1% on the liquid-phase composition, 5% on the solid-phase composition, and 5−10% on the solid fraction.

The precipitate (P) recovered is composed by the solid phase (S) and important quantities of liquid (L) that remain entrapped in the crystals after the filtration. It is thus impossible to assess directly the composition of the solid phase after the filtration. Only the composition of the liquid phase (L) and the precipitate (P) can be determined directly. Because the unsaturated fatty acid esters have melting points much lower than the corresponding saturated fatty acid esters, they will not crystallize at the temperatures used on this study, and thus, the portion of liquid entrapped in the crystals of the precipitate can be determined from the quantity of unsaturated fatty esters present in the precipitate. Because the exact composition of the liquid phase is known from chromatography, it is possible to calculate the fraction of entrapped liquid, c, as

$$c = \frac{W^{\mathrm{P}}_{\mathrm{C18:1}} + W^{\mathrm{P}}_{\mathrm{C18:2}}}{W^{\mathrm{L}}_{\mathrm{C18:1}} + W^{\mathrm{L}}_{\mathrm{C18:2}}} \quad (1)$$

where W is the mass fraction of the compounds obtained from the chromatographic analysis and P and L stand for the precipitate and liquid fractions. Using the value of this fraction c, it is possible to estimate the composition of the various compounds i present in the solid phase, S, as

$$W_i^{\mathrm{S}} = \frac{W_i^{\mathrm{P}} - cW_i^{\mathrm{L}}}{1-c} \quad (2)$$

The fraction of the initial biodiesel sample that crystallized, X^{S}, can be obtained from a mass balance to any of the compounds present but is ideally estimated from the concentration of any of the unsaturated fatty acid esters on both the original biodiesel, BD, and the concentration in the liquid phase, L, under the conditions studied as

$$X^{\mathrm{S}} = \frac{W_i^{\mathrm{L}} - W_i^{\mathrm{BD}}}{W_i^{\mathrm{L}}} \quad (3)$$

This experimental methodology allows for an easy measurement of the composition of the liquid, W^{L}, and solid, W^{S}, phases

(26) Costa, M. C.; Krahenbuhl, M. A.; Meirelles, A. J. A.; Daridon, J. L.; Pauly, J.; Coutinho, J. A. P. *Fluid Phase Equilib.* **2007**, *253*, 118–123.
(27) Lopes, J. C. A.; Boros, L.; Krähenbühl, M. A.; Meirelles, A. J. A.; Daridon, J. L.; Pauly, J.; Marrucho, I. M.; Coutinho, J. A. P. *Energy Fuels* **2008**, *22*, 747–752.
(28) Boros, L.; Batista, M. L. S.; Vaz, R. V.; Figueiredo, B. R.; Fernandes, V. F. S.; Costa, M. C.; Krahenbuhl, M. A.; Meirelles, A. J. A.; Coutinho, J. A. P. *Energy Fuels* **2009**, *23*, 4625–4629.
(29) Kerschbaum, S.; Rinke, G.; Schubert, K. *Fuel* **2008**, *87*, 2590–2597.
(30) Lee, I.; Johnson, L. A.; Hammond, E. G. *J. Am. Oil Chem. Soc.* **1996**, *73*, 631–636.
(31) Dunn, R. O.; Schockley, M. W.; Bagby, M. O. SAE Tech. Pap. 971682, 1997.
(32) Dauphin, C.; Daridon, J. L.; Coutinho, J. A. P.; Baylere, P.; Pontin-Gautier, M. *Fluid Phase Equilib.* **1999**, *161*, 135–151.
(33) Pauly, J.; Daridon, J. L.; Coutinho, J. A. P. *Fluid Phase Equilib.* **2001**, *187*, 71–82.
(34) Pauly, J.; Daridon, J. L.; Coutinho, J. A. P. *Fluid Phase Equilib.* **2004**, *224*, 237–244.
(35) Pauly, J.; Daridon, J. L.; Coutinho, J. A. P.; Dirand, M. *Fuel* **2005**, *84*, 453–459.
(36) Coutinho, J. A. P.; Gonçalves, C.; Marrucho, I. M.; Pauly, J.; Daridon, J. L. *Fluid Phase Equilib.* **2005**, *233*, 29–34.

Table 2. Thermophysical Properties of Saturated Fatty Acid Methyl Esters

	T_{fus} (K)	$\Delta_{fus}H$ (kJ mol^{-1})	$\Delta_{vap}H$ (kJ mol^{-1})
C16:0	302.59	56.85	96.58
C18:0	311.45	64.84	105.92

as well as the fraction of crystallized material, X^S, as a function of the temperature.

3. Thermodynamic Model

The precipitation of solids in biodiesel at low temperatures is described using an approach previously proposed by us for alkane mixtures[10−25] and also applied to fatty acids[26] and fatty acids methyl and ethyl esters[27,28] with success.

The solid−liquid equilibrium can be described by an equation relating the composition of component i in the solid and liquid phases with their non-ideality and the thermophysical properties of the pure component[37]

$$\ln\frac{x_i^s\gamma_i^s}{x_i^l\gamma_i^l} = \frac{\Delta_{fus}H_i}{RT_{fus,i}}\left(\frac{T_{fus,i}}{T}-1\right) - \frac{\Delta_{fus}C_{p,i}(T_{fus,i})}{R}\left(1-\frac{T_{fus,i}}{T}+\ln\frac{T_{fus,i}}{T}\right) \quad (4)$$

where γ_i is the activity coefficient of the compound, x_i is its mole fraction, $\Delta_{fus}H(T_{fus})$ is the molar enthalpy of fusion of the pure solute at the melting temperature T_{fus}, and $\Delta_{fus}C_{p,i}(T_{fus,i})$ is the molar heat capacity change upon fusion at fusion temperature T_{fus}. The heat capacity change upon fusion is usually regarded as being independent of the temperature, and the term in parentheses multiplied by $\Delta_{fus}C_{p,m}$ is often considered as being small, because the opposite signs inside the parentheses lead to near cancellation.[38] This term was thus neglected on the calculations. The thermophysical properties of the crystallizing saturated fatty acid esters used were obtained from correlations developed in a previous work[27] and are reported in Table 2.

Because the major compounds of a biodiesel are fatty acid esters of similar size and nature, the liquid phase may be treated as an ideal solution. Using eq 1, along with a multiphase flash algorithm, the composition and amount of the phases in equilibrium can be calculated if a model for the non-ideality of the solid phases is available. Because of its simplicity and robustness, the algorithm of resolution of the Rachford−Rice equations proposed by Leibovici and Neoschil[39] was used in the calculations.

The solid-phase non-ideality is described by the most recent version of the predictive UNIQUAC model.[15] The UNIQUAC model can be written as

$$\frac{g^E}{RT} = \sum_{i=1}^{n} x_i \ln\left(\frac{\Phi_i}{x_i}\right) + \frac{Z}{2}\sum_{i=1}^{n} q_i x_i \ln\frac{\theta_i}{\Phi_i} - \sum_{i=1}^{n} x_i q_i \ln\left[\sum_{j=1}^{n}\theta_j \exp\left(-\frac{\lambda_{ij}-\lambda_{ii}}{q_i RT}\right)\right] \quad (5)$$

with

$$\Phi_i = \frac{x_i r_i}{\sum_j x_j r_j} \text{ and } \theta_i = \frac{x_i q_i}{\sum_j x_j q_j} \quad (6)$$

On this version of predictive UNIQUAC, the structural parameters, r_i and q_i, are obtained from the UNIFAC parameter table.[40]

The predictive local composition concept[10−15] allows for the estimation of the interaction energies, λ_{ij}, used by these models without fitting to experimental data. The pair interaction energies between two identical molecules are estimated from the heat of sublimation of the pure component

$$\lambda_{ii} = -\frac{2}{Z}(\Delta_{sub}H_i - RT) \quad (7)$$

where Z is the coordination number with a value of 10 as in the original UNIQUAC model.[15,41] The heats of sublimation are calculated at the melting temperature of the pure component as

$$\Delta_{sub}H = \Delta_{vap}H + \Delta_{fus}H \quad (8)$$

The pair interaction energy between two non-identical molecules is given by

$$\lambda_{ij} = \lambda_{ji} = \lambda_{jj}(1+\alpha_{ij}) \quad (9)$$

where j is the ester with the shorter chain of the pair ij. The interaction parameter α_{ij} allows for the tuning of the non-ideality of the solid solution. In this work, three approaches to the solid-phase non-ideality will be evaluated: assuming $\alpha_{ij} = 0$ (UNIQUAC), as was previously performed for alkanes,[10−25] using $\alpha_{ij} = -0.05$ (UNIQUAC − 0.05), a value similar to that used on the description of the phase diagrams of fatty acids[26] and fatty acid esters,[27] and finally, assuming that there is no solid solution formation and each compound crystallizes as a pure crystal (no solution). This last situation corresponds to an infinite value of the solid-phase activity coefficient that within the framework of predictive UNIQUAC can be achieved with a value of α_{ij} larger than −0.25.

The solid−liquid equilibrium model used in this work is thus a purely predictive model that uses only pure component properties for the calculation of the phase equilibria. The three versions evaluated here will be used to predict the low-temperature behavior of the three biodiesels studied in this work.[42]

4. Results and Discussion

The experimental methodology used on this work provides direct information about the composition of the liquid phase. The compositions of the solid phase are estimated from the composition of the liquid phase and the precipitate according to eqs 1 and 2. The fraction of solids crystallizing from the biodiesel at each temperature is obtained from the differences between the concentrations of the unsaturated fatty acid esters on the original biodiesel and on the liquid phase according to eq 3. It follows that the uncertainty associated with the solid-phase compositions and the solid fractions is consequently larger than that of the liquid phase, which is just the uncertainty associated with the GC analysis. The compositions

(37) Prausnitz, J. M.; Lichtenthaler, R. N.; Azevedo, E. G. *Molecular Thermodynamics of Fluid-Phase Equilibria*, 3rd ed.; Prentice Hall: New York, 1999.
(38) Coutinho, J. A. P.; Andersen, S. I.; Stenby, E. H. *Fluid Phase Equilib.* **1995**, *103*, 23–29.
(39) Leibovici, C. F.; Neoschil, J. *Fluid Phase Equilib.* **1995**, *112*, 217–221.
(40) Larsen, B. L.; Rasmussen, P.; Fredenslund, A. *Ind. Eng. Chem. Res.* **1987**, *26*, 2274–2286.
(41) Abrams, D. S.; Prausnitz, J. M. *AIChE J.* **1975**, *21*, 116–128.
(42) The program used to perform the calculations reported on this work can be obtained from the authors.

Table 3. Composition (wt %) of the Solid and Liquid Phases in Equilibrium as a Function of the Temperature for BDA

	liquid phase				solid phase		
temperature (K)	C16:0	C18:0	C18:1	C18:2	C16:0	C18:0	solid fraction
265.65	4.57	1.05	33.82	59.54	81.08	18.92	15.28
268.15	5.23	1.06	33.84	59.10	80.23	19.77	14.95
270.65	6.60	1.43	33.19	57.95	80.21	19.79	13.47
273.15	8.34	1.86	31.98	56.77	80.91	19.09	11.15
275.65	10.91	2.75	30.91	54.42	82.61	17.39	7.47

Table 4. Composition (wt %) of the Solid and Liquid Phases in Equilibrium as a Function of the Temperature for BDB

	liquid phase				solid phase		
temperature (K)	C16:0	C18:0	C18:1	C18:2	C16:0	C18:0	solid fraction
260.65	2.63	0.87	58.45	37.06	65.90	34.10	5.62
263.15	3.58	1.21	57.33	36.39	62.04	37.96	3.83
265.65	4.11	1.58	57.04	36.29	64.54	35.46	3.44
268.15	5.52	2.22	55.60	35.02	36.45	63.55	2.45
270.15	5.32	2.19	56.39	34.76	10.97	89.03	2.11

Table 5. Composition (wt %) of the Solid and Liquid Phases in Equilibrium as a Function of the Temperature for BDC

	liquid phase				solid phase		
temperature (K)	C16:0	C18:0	C18:1	C18:2	C16:0	C18:0	solid fraction
260.65	4.20	1.23	25.86	68.71	71.86	28.14	11.05
263.15	5.61	1.84	25.32	66.87	71.92	28.08	9.14
265.65	6.00	1.98	25.07	66.34	70.98	29.02	8.23
268.15	6.73	2.35	24.94	65.46	72.18	27.82	7.19
270.65	10.70	3.95	22.97	61.40	71.27	28.73	0.50

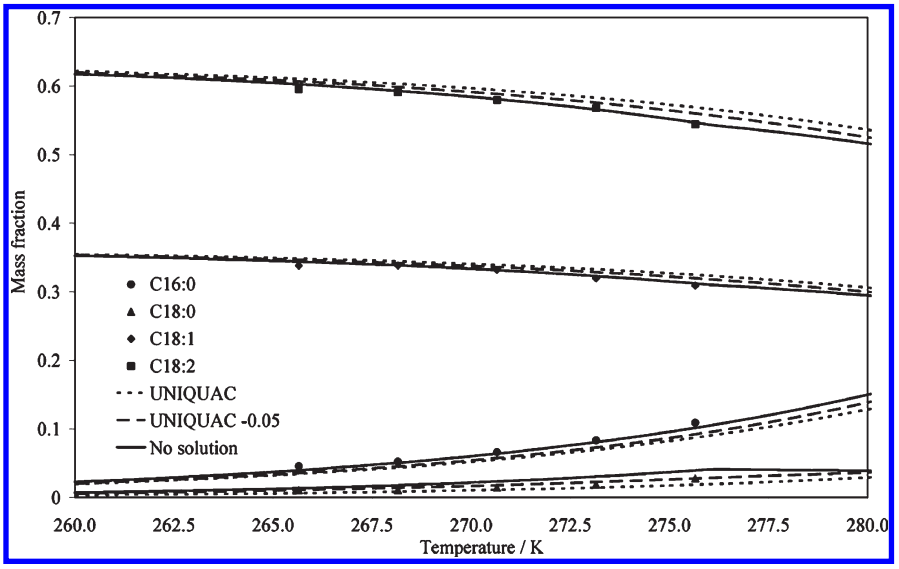

Figure 1. Liquid-phase composition for BDA.

of the liquid and solid phases along with the solid fraction formed are reported on Tables 3−5 at the various temperatures studied for each of the biodiesels used on this work. These values along with the predictions achieved by the three studied models are presented in Figures 1−9.

Because the lowest temperature studied was 260.65 K and the melting points of the unsaturated fatty acid esters present on the biodiesel are lower than this value, it was admitted that these compounds did not crystallize under the conditions used in this work. The solid phase is thus composed solely by the saturated fatty acid methyl esters, methyl palmitate (C16:0) and methyl stearate (C18:0). The temperature dependency of the liquid-phase compositions observed for all of the biodiesels is similar, as shown in Figures 1, 4, and 7. As the temperature decreases, the saturated esters crystallize and then the liquid phase becomes depleted on the saturated esters and enriched on the unsaturated esters. This results in an increase of the unsaturated esters concentration at low temperatures, while the saturated esters show the opposite behavior with a decrease in the concentration with temperature. In what concerns the description of the liquid-phase compositions, the three models adopted have quite similar performances, providing a description of the data that is essentially within their experimental uncertainty.

The solid-phase compositions presented in Figures 2, 5, and 8 display a richer and more complex behavior, becoming a more stringent test to the models. Although the models predict a similar solid-phase composition at temperatures 5−10 K lower than

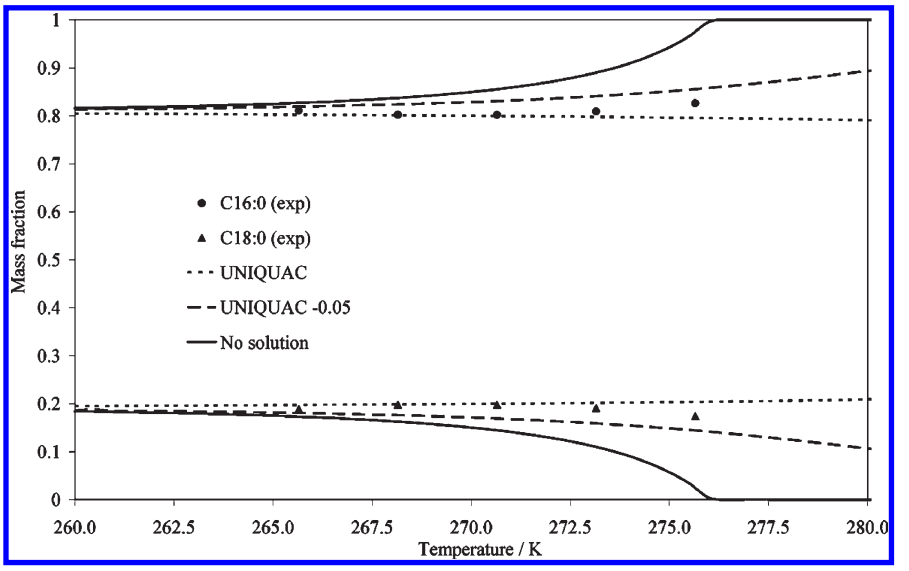

Figure 2. Solid-phase composition for BDA.

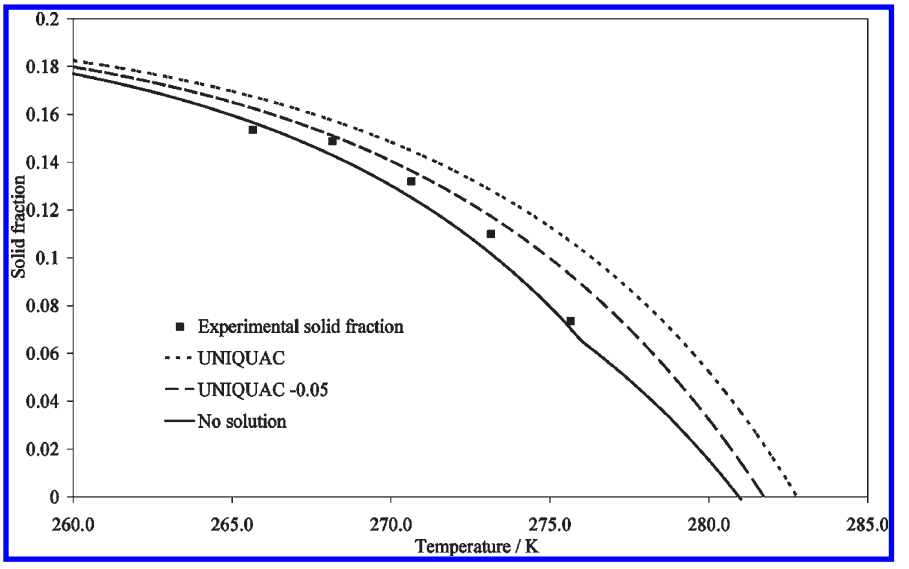

Figure 3. Dependence with the temperature of the fraction of precipitated solid material for BDA.

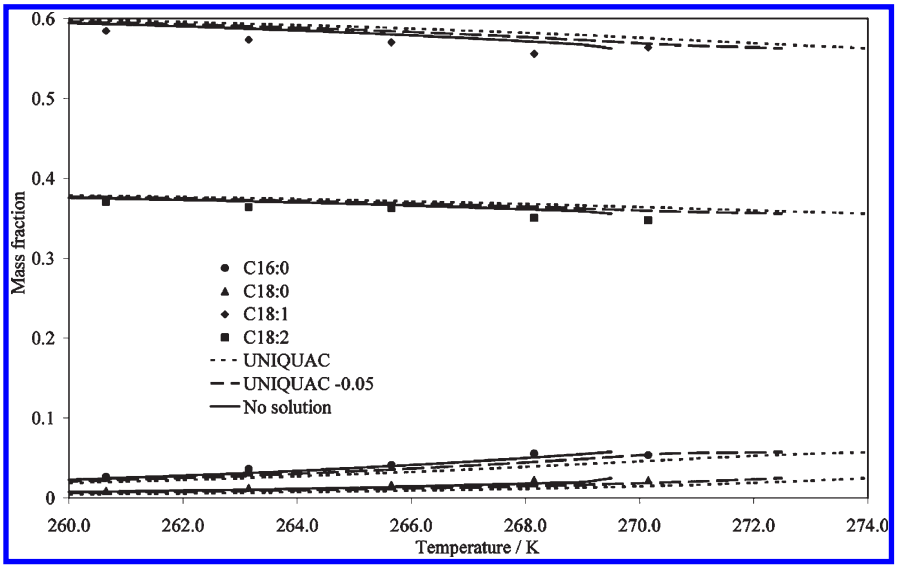

Figure 4. Liquid-phase composition for BDB.

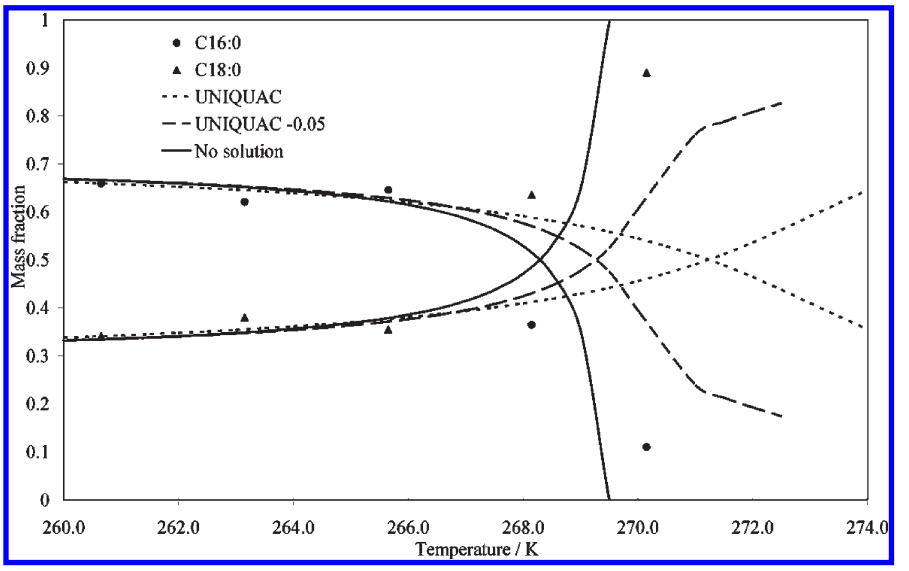

Figure 5. Solid-phase composition for BDB.

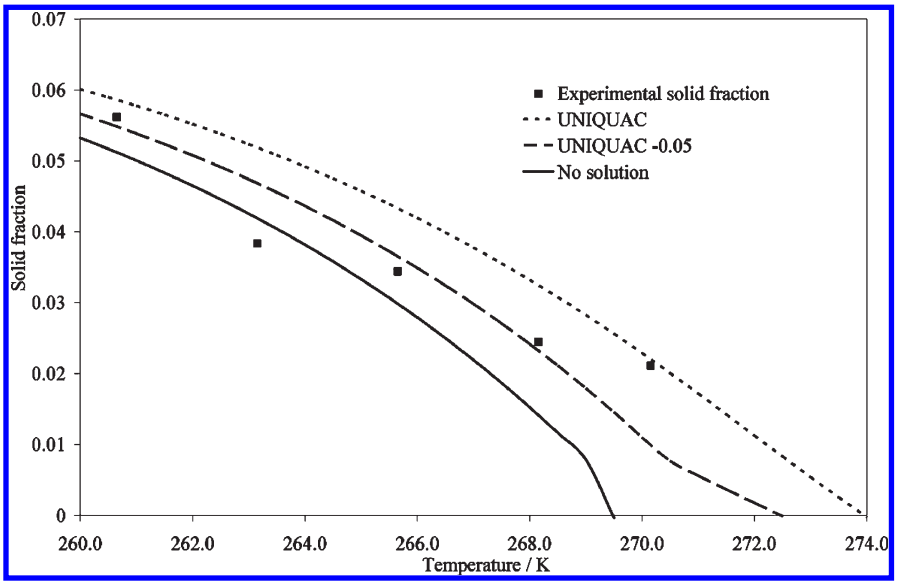

Figure 6. Dependence with the temperature of the fraction of precipitated solid material for BDB.

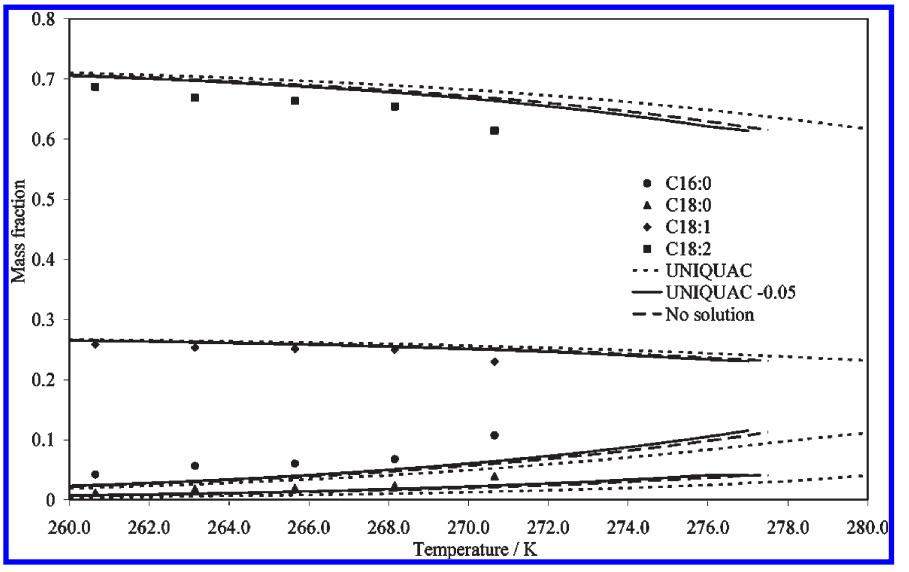

Figure 7. Liquid-phase composition for BDC.

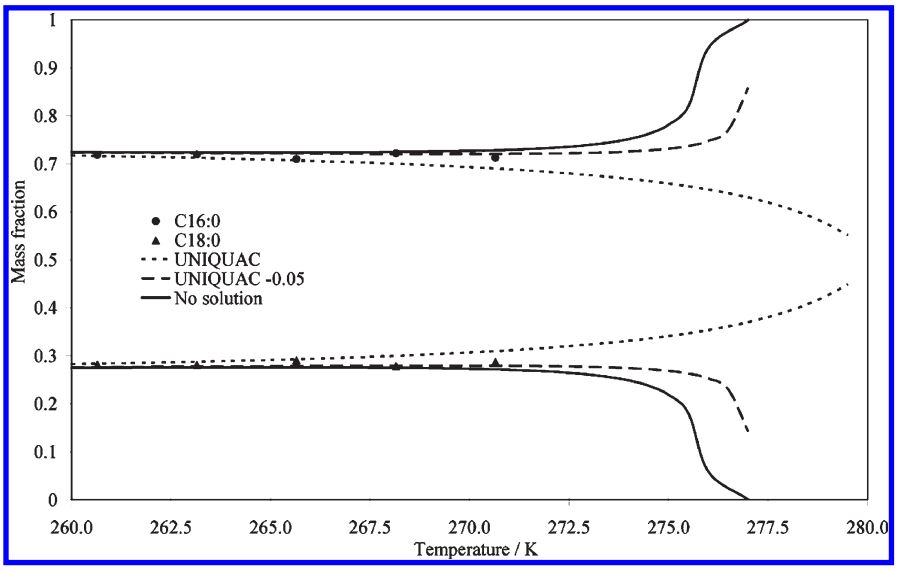

Figure 8. Solid-phase composition for BDC.

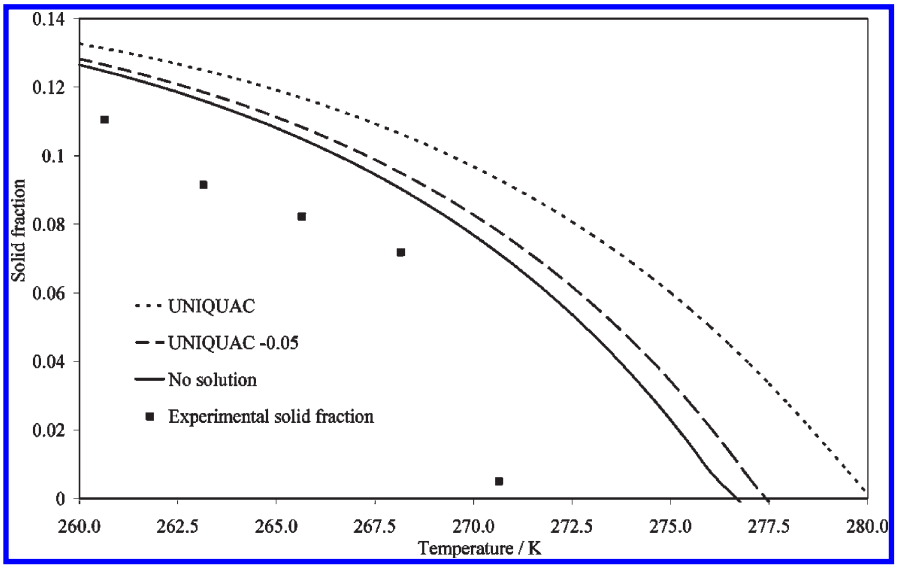

Figure 9. Dependence with the temperature of the fraction of precipitated solid material for BDC.

the CP, close to it they display a very different behavior. While the predictive UNIQUAC model with $\alpha_{ij} = 0$ (UNIQUAC) predicts that both saturated esters crystallize simultaneously, as expected from the formation of a solid solution, the model assuming that each ester crystallizes independently (no solution) starts with the crystallization of just one of the esters and, as the temperature decreases and the ratio between the stearate and palmitate esters reaches the eutectic point of the mixture, they both start to crystallize, although as independent solid phases. This produces some interesting features on the phase equilibria predicted by the no solution model, such as a small increase on the concentration of the methyl stearate on the liquid phase below the CP and down to 276 K for BDA, while the methyl palmitate crystallizes alone.

The kinks observed on the solid fraction lines predicted by this model and reported in Figures 3, 6, and 9 can also be assigned to the change of regimen of crystallization of a single ester to the simultaneous crystallization of two esters. In any case, these behaviors would be too subtle to be observed on the experimental data to test the model validity. The predictive UNIQUAC model with $\alpha_{ij} = -0.05$ (UNIQUAC − 0.05) presents an intermediate behavior between these two extremes. While it clearly favors the crystallization of one of the esters over the other at the CP, it still predicts nevertheless that there is always some degree of co-crystallization. This allows for the correct description of the decrease in methyl palmitate and increase in methyl stearate concentrations as the temperature decreases observed in BDA. The UNIQUAC model predicts the opposite behavior for all of the studied biofuels, while the no solution model, although qualitatively correct, overestimates this composition change. This change in the solid-phase composition is particularly visible for BDB, shown in Figure 5. Because in BDB the methyl palmitate/methyl stearate ratio is much lower than in the two other fuels, the crystallization will start on the opposite side of the eutectic point than observed in BDA and BDC. This originates that at the CP it will be the methyl stearate rather than the methyl palmitate that dominates in the solid phase. This peculiar behavior is rather clear in the experimental data, with an inversion of the dominant ester in the solid phase as the temperature decreases.

Although all of the models can qualitatively describe the change in the dominant ester present in the solid phase, the UNIQUAC model fails to adequately describe it, while the two other models provide a fair description of the concentration inversion. On BDC, presented in Figure 8, the UNIQUAC model again fails to provide a description of the qualitative trend observed in the solid-phase compositions. The other two models show no differences within the experimental temperature range studied.

The crystallization differences around the CP, along with the differences on the estimation of the CP itself, generate important differences on the solid fractions predicted by the three models studied on this work, reported in Figures 3, 6, and 9. The solid fraction, as well as the CP estimation, decreases with the increasing non-ideality of the solid phase. In all cases, the solid fractions predicted by the UNIQUAC model are larger than those estimated by the UNIQUAC − 0.05, and these are larger than those obtained from the no solution model. It is clear that the UNIQUAC model overestimates the solid fractions measured. Given the quality of the experimental data measured for the solid fractions, it is not possible to clearly identify which of the two other models is the best because both describe the data within its experimental uncertainty.

A global analysis of the data suggests that both the UNIQUAC − 0.05 and the no solution model can provide an adequate description of the phase equilibrium data of biodiesels below the CP of the fuel. The UNIQUAC − 0.05 model is probably superior, with a better description of the CP and the solid-phase composition. A more extensive set of data and higher quality seems to be required to reach a final conclusion.

5. Conclusions

This work reports experimental data for the solid−liquid-phase equilibria of three commercial, non-additive biodiesels at temperatures ranging from 260 to 275 K. A thermodynamic framework able to describe these multiphase systems is presented. Two versions of the predictive UNIQUAC model along with a model assuming complete immiscibility of the compounds in the solid phase are evaluated against the experimental data measured. It is shown that both the predictive UNIQUAC model with $\alpha_{ij} = -0.05$ (UNIQUAC − 0.05) and a model assuming complete immiscibility on the solid phase are capable of providing an adequate representation of the phase equilibria for these systems below their CPs.